Available online at www.sciencedirect.com
SCIENCE DIRECT®
Tectonophysics 372 (2003) 1–21
TECTONOPHYSICS
www.elsevier.com/locate/tecto

Evolution of mica fish in mylonitic rocks

S.M. ten Grotenhuis[a,b,*], R.A.J. Trouw[c], C.W. Passchier[b]

[a] Faculty of Earth Sciences, Utrecht University, The Netherlands
[b] Tectonophysics, Institut für Geowissenschaften, Mainz University, Germany
[c] Federal University of Rio de Janeiro, Departamento de Geologia, Brazil

Received 28 August 2002; accepted 13 June 2003

Abstract

Mineral fish are lozenge-shaped porphyroclasts, single crystals in a finer grained matrix, which occur in ductile shear zones and which are commonly used as shear sense indicators. Mineral fish of biotite, tourmaline, K-feldspar, garnet, hypersthene and quartz occur in mylonites but most common are white mica fish. These mica fish can be subdivided into six morphological groups that develop by different mechanisms determined by different initial shapes and orientations. The principal mechanisms of formation are intracrystalline deformation combined with rigid body rotation. Concomitant selective grain size reduction occurs by recrystallisation, cataclastic separation, pressure solution and diffusional mass transfer. Microboudinage has been proposed for the breakdown of large mica fish into smaller ones but many mica fish undergo shortening rather than extension along their long axes. Evidence is presented for an alternative process in which the tips of mica fish are isoclinally folded and then break off along the hinge of these microfolds. All the presented fish-shaped porphyroclasts or mineral fish have a specific shape-preferred orientation with their long axis at a small antithetic angle with respect to the foliation. They represent a special group of objects with a stable orientation due to flow partitioning into narrow shear bands.

Keywords: Shear zones; Mylonite; Microstructure; Mica fish; Kinematic indicators

1. Introduction

Mylonites are rocks that develop dominantly by strong ductile deformation in zones of intense non-coaxial flow (Bell and Etheridge, 1973). Many mylonites contain porphyroclasts with a significantly larger grain size than the matrix material. Porphyroclasts are thought to develop because they are more resistant to deformation and dynamic recrystallisation than their matrix. During deformation, these porphyroclasts can develop into sense-of-shear markers, such as mantled porphyroclasts (Passchier and Simpson, 1986; Hanmer, 1990), clasts with asymmetric strain shadows and "fish" (Fig. 1; Eisbacher, 1970; Lister and Snoke, 1984). Polycrystalline objects of similar shape such as foliation fish, asymmetric shear-band shaped boudins and sigmoidal veins, are not discussed in this paper.

Mantled porphyroclasts consist of a large monocrystalline core mantled by recrystallised material derived from this core, constituting the wings of the object (Fig. 1a). Asymmetric strain shadows may show similar sigmoidal structures, but here the core and shadows are composed of different minerals

* Corresponding author. HPT-Laboratory, Faculty of Earth Sciences, Utrecht University, P.O. Box 80021, 3508 TA Utrecht, The Netherlands. Tel.: +31-30-2531177.
E-mail address: saskiatg@geo.uu.nl (S.M. ten Grotenhuis).

0040-1951/$ - see front matter © 2003 Elsevier B.V. All rights reserved.
doi:10.1016/S0040-1951(03)00231-2

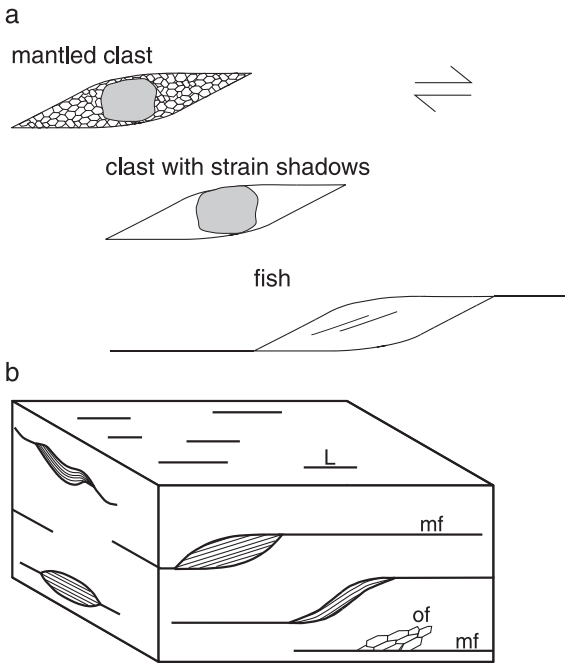

Fig. 1. (a) Examples of sigmoidal microstructures: mantled porphyroclast, porphyroclast with strain shadows and fish, lens-shaped single crystals. Black lines extending from the tips of the fish represent the trails of fine-grained mica. (b) Schematic drawing of mica fish and the trails of mica fragments, in relationship with mylonitic foliation (mf), oblique foliation (of) and stretching lineation (l).

(Fig. 1a). Fish are lozenge or lens-shaped single crystals ending in sharp tips, generally attached to trails consisting of small fragments of the same mineral stretching from the tips into the wall rock (Fig. 1a). Frequently, the trails in these structures show stair-stepping; they are parallel to each other, but offset across the object core (Fig. 1a; Passchier, 1994).

Fish-shaped structures are most common in white mica, but have also been described for other minerals, e.g. leucoxene (Oliver and Goodge, 1996), garnets (Ji and Martignole, 1994; Azor et al., 1997; Pennacchioni et al., 2001), quartz in a calcite matrix (Bestmann, 1999, Bestmann et al., 2000), sillimanite and plagioclase (Pennacchioni et al., 2001), hornblende, clinopyroxene and olivine (Mancktelow et al., 2002). In our experience, practically any mineral species capable of forming porphyroclasts in mylonites can develop oblique lens-shaped porphyroclasts, comparable to mica fish. We therefore propose to use the term ‘‘fish’’ for any type of oblique lens-shaped porphyroclast. All these shapes display characteristic angular tips that often grade into trails of small grains of the same mineralogy.

White mica fish (further referred to as mica fish) are relatively common in mylonitised gneisses and in mylonites derived from micaceous quartzites (Eisbacher, 1970; Lister and Snoke, 1984). They have been shown empirically to be reliable shear sense indicators (e.g. Lister and Snoke, 1984), based on their asymmetrical shape and stair stepping of the trails (Fig. 1b). Although the importance of mica fish has been widely recognised (e.g. Eisbacher, 1970; Simpson and Schmid, 1983; Lister and Snoke, 1984; Passchier and Trouw, 1996), their genesis and kinematic significance remain relatively unexplored.

Analytical theory (Jeffery, 1922; Ghosh and Ramberg, 1976) predict that elliptical rigid particles embedded in an isotropic, linear viscous matrix undergoing non-coaxial flow should develop a stable orientation when their aspect ratio exceeds a critical limit which depends on the kinematic vorticity of the flow, while less elongate grains rotate continuously, although with oscillating velocity. Such ‘‘stable grains’’ are synthetically orientated with respect to the mylonitic foliation, and this kind of behaviour has been observed, in experiments and in nature, for mantled porphyroclasts (Passchier, 1987). Even if an initial preferred orientation existed in a population of objects, at least part of this population will be lying oblique to the final preferred orientation due to differential rotation. Mica fish show an entirely different orientation pattern. They show a strong shape-preferred orientation with the longest dimension inclined at a small antithetic angle with respect to the main mylonitic foliation (Fig. 1b, e.g. Lister and Snoke, 1984; ten Grotenhuis et al., 2002; Mancktelow et al., 2002). This preferred orientation therefore suggests that mica fish are in a stable orientation independent of strain intensity, but it cannot be explained by the behaviour of rigid objects in a homogeneously deforming isotropic matrix material (Pennacchioni et al., 2001; ten Grotenhuis et al., 2002; Mancktelow et al., 2002).

Based on field and thin section observations, Lister and Snoke (1984) claimed that quartzites with mica fish are a special type of S–C mylonite, a structural setting in which two foliations are developed: C-

surfaces related to displacement discontinuities and S-surfaces related to the accumulation of finite strain (Berthé et al., 1979). In quartz-mica rocks, Lister and Snoke (1984) define the C-surfaces as trails of mica fragments forming the main mylonitic foliation; each C-plane is believed to be the result of a microscopically thin displacement discontinuity. The S-surface is defined by an oblique foliation of quartz in the matrix, mainly characterised by a grain shape-preferred orientation. This oblique foliation is formed when the matrix is dynamically recrystallised during deformation (Means, 1981). According to Lister and Snoke (1984), the mica fish in these rocks result from microboudinage of pre-existing large (white) mica grains by brittle and crystal-plastic processes.

Recently, ten Grotenhuis et al. (2002) and Mancktelow et al. (2002) have reported unexpected rotational behaviour of rigid elongated monoclinic objects in experimental shear zones. Experiments by ten Grotenhuis et al. (2002) have demonstrated that elongated rigid objects *can* reach a stable position at a small antithetic angle to the flow plane, very similar to the one observed in natural examples of mica fish. In the experiments of ten Grotenhuis et al. (2002), a granular material with low cohesion and Mohr–Coulomb type behaviour is used as the matrix. The behaviour or the central object was attributed to small-scale localisation of slip in the matrix and along the sides of the object. Although the stable orientations obtained in these experiments vary for different vorticity numbers, in all experiments, they were related to the development of small-scale strain localisation along micro-shear zones. Mancktelow et al. (2002) obtained comparable results for particles with slipping particle-matrix interfaces in a homogeneous Newtonian matrix. They concluded that slip or concentrated shear on rigid particle boundaries is a potential mechanism to explain the observed strain-insensitive shape-preferred orientation of some natural porphyroclasts in high strain mylonites. In both sets of experiments, the rotation direction depends on the initial orientation of the objects; objects initially perpendicular to the shear direction rotate synthetically, and objects parallel to the shear direction rotate antithetically. The final stable orientation for the objects is in both sets of experiments at a small antithetic angle to the flow plane. A small anthithetic angle has also been observed for rigid elliptical objects in very narrow shear zones (Marques and Cobbold, 1995; Marques and Coelho, 2001).

The objective of this paper is to provide data on the geometry and orientation of natural fish-shaped grains in order to strengthen the basis for study of their evolution. The final shape of fish may depend on many controlling factors, such as strain intensity, strain rate, temperature, pressure, fluid composition and mineral content of the host rock. In order to put constraints on these factors, we concentrated on common white mica fish and present detailed morphological data of approximately 1500 muscovite fish from 28 thin sections. We also investigated samples with fish composed of biotite, tourmaline, K-feldspar, garnet, hypersthene and quartz, in 75 thin sections from several locations. Their morphological aspects are described and compared to the white mica fish, in order to assess whether the same deformation processes were active, and whether a common evolution can be deduced for these microstructures.

2. Morphology of mica fish

The studied samples of mylonitic micaceous quartzite are from an outcrop along the highway that links the cities of Caxambu and Cambuquira, approximately 5 km south of Conceição do Rio Verde, Southern Minas Gerais State, Brazil (0498972E/7574231N). The quartzites containing the mica fish are clearly of metasedimentary origin and belong to the lower unit of the Neoproterozoic Andrelândia Depositional Sequence (Trouw et al., 1983; Paciullo et al., 1993; Ribeiro et al., 1995) that consists of stratified paragneisses with intercalated quartzites and schists. The outcrop is situated in an ENE trending subvertical dextral shear zone of about 500 m thickness.

The amount of muscovite in the mylonitised quartzites varies between about 10 and 20 vol.%. Non-mylonitic micaceous quartzites outside the shear zone contain similar proportions of muscovite, but with larger grain size and more rectangular shapes (Fig. 2), demonstrating that the mica fish are porphyroclasts that decreased in size during the deformation. It seems reasonable to assume that the mylonitised quartzites had a strong schistosity before mylonitisation, because all metasedimentary rocks in the region have such a fabric, due to combined D_1/D_2 deforma-

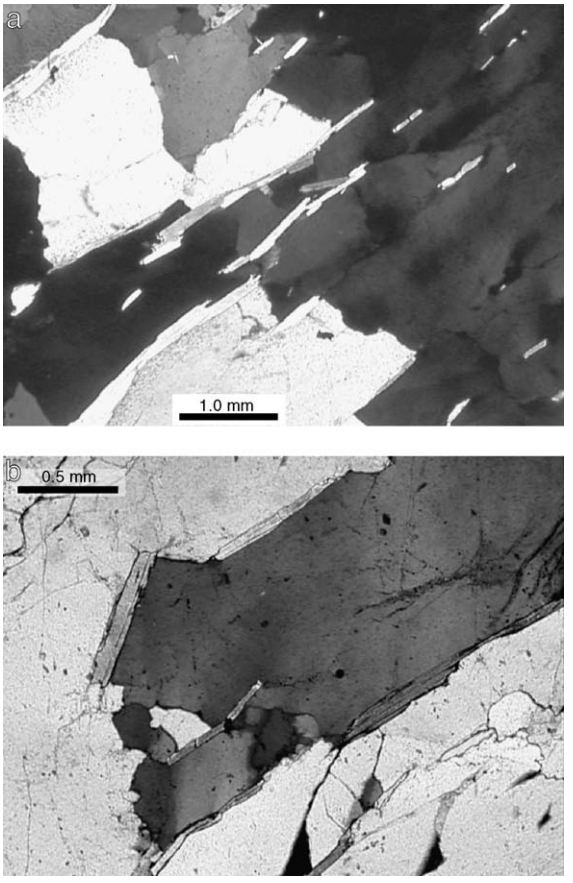

Fig. 2. Photomicrographs of the micaceous quartzites with rectangular shaped muscovite grains from a location outside the mylonite zone.

tion, both predating the shear zone that is ascribed to D_3 (Trouw et al., 2000). This schistosity was than rotated into parallelism with the shear zone. The mylonitic quartzites contain a single strong mylonitic foliation accompanied by a penetrative stretching lineation, defined by the shape-preferred orientation of quartz aggregates, single quartz grains and muscovite grains. The metamorphic grade during deformation is estimated as upper greenschist facies according to the metamorphic mineral association biotite + chlorite + garnet + muscovite + quartz, which was apparently stable during mylonitisation.

In three dimensions, the mica fish usually have a flake or disc-shape, and in some cases are bent or folded (Fig. 1b). In the plane parallel to the foliation, they are only slightly elongated in the direction of the

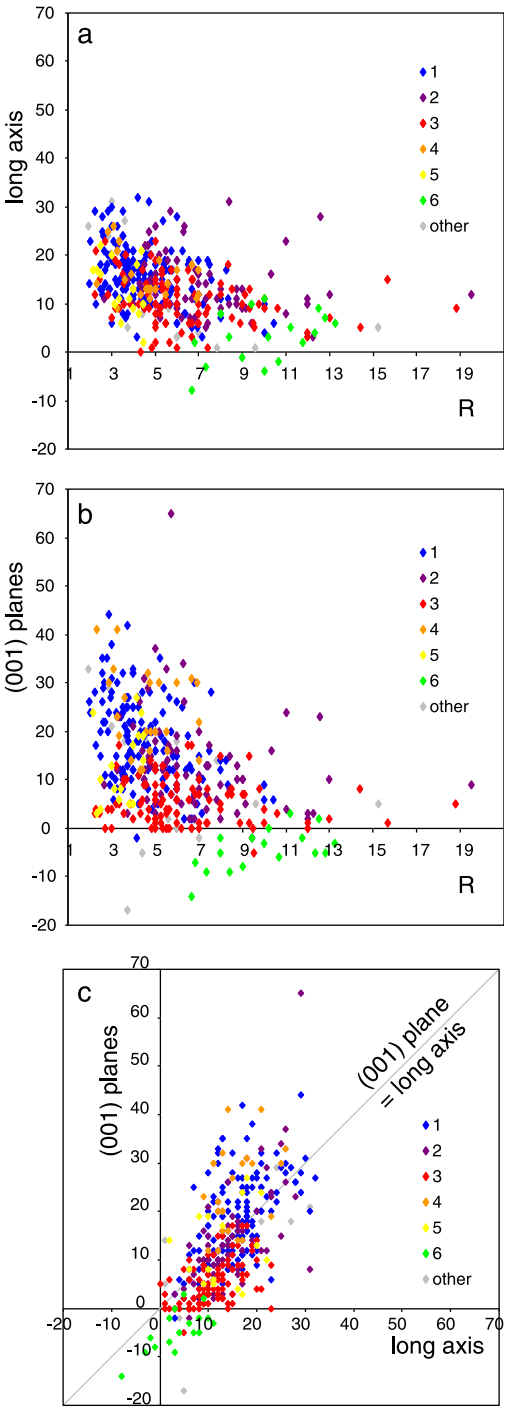

Fig. 3. (a) Orientation of the long axes vs. aspect ratio (R), (b) (001) planes vs. aspect ratio (R) and (c) orientation of the long axis vs. (001) planes with respect to the mylonitic foliation of 400 mica fish.

stretching lineation. The length of the longest axis of mica fish is up to 4 mm. In the plane parallel to the stretching lineation and perpendicular to the foliation, the mica fish are elongated and the average aspect ratio of 400 measured mica fish is 5.7 (Fig. 3a). The matrix surrounding the mica fish consists of fine-grained quartz with an oblique foliation, which makes an average angle of 34° with the mylonitic foliation. Trails of very small mica fragments extend from the tips of the mica fish into the matrix (Fig. 1b). These 10–100 μm wide trails define the mylonitic foliation. They usually show very clear 'stair-stepping' (Lister and Snoke, 1984; Passchier et al., 1993; Passchier and Trouw, 1996) across each mica fish. Mica fish are inclined to the mylonitic foliation in the same direction as the oblique foliation. The angle between the long axes of 400 measured mica fish and the mylonitic foliation has a mean value of 13° (Fig. 3a), whereas the angle between the basal plane (001) and the mylonitic foliation has a mean value of 11° (Fig. 3b).

The morphology of mica fish as seen in thin sections cut parallel to the lineation and perpendicular to the foliation permits a subdivision into several groups based on shape and orientation of lattice planes. These groups are not meant as a definite new nomenclature, but rather as a provisional subdivision until more is known about the generation of fish. The subdivision is based on samples from different locations across the shear zone. Most common is a lenticular shape (Figs. 4 and 5a) with curved sides, usually ending in sharp tips: 33% of the mica fish belong to this group, labelled group 1. The orientation of the lattice planes is usually parallel or at a small angle to the long axes of these fish (Fig. 3). In some of the lenticular-shaped fish, the lattice planes converge on an internal discontinuity at one or both tips. Also common are mica fish whose tips deflect into the plane of the mylonitic foliation (19%, Fig. 4). The lattice planes of these fish (group 2) are typically curved at the tips. Fish with a parallelogram-shape form groups 3 and 4. The sides of these fish are straight compared to the lenticular ones. The longest side of this type of fish is typically sub-parallel to the mylonitic foliation, and lattice planes are usually parallel to this side (group 3: 25%, Figs. 3, 4 and 5c). Less common are mica fish with a parallelogram shape in which lattice planes are parallel to the short side (group 4: 8%, Figs. 3, 4 and 5d). Group 5, representing 5% of

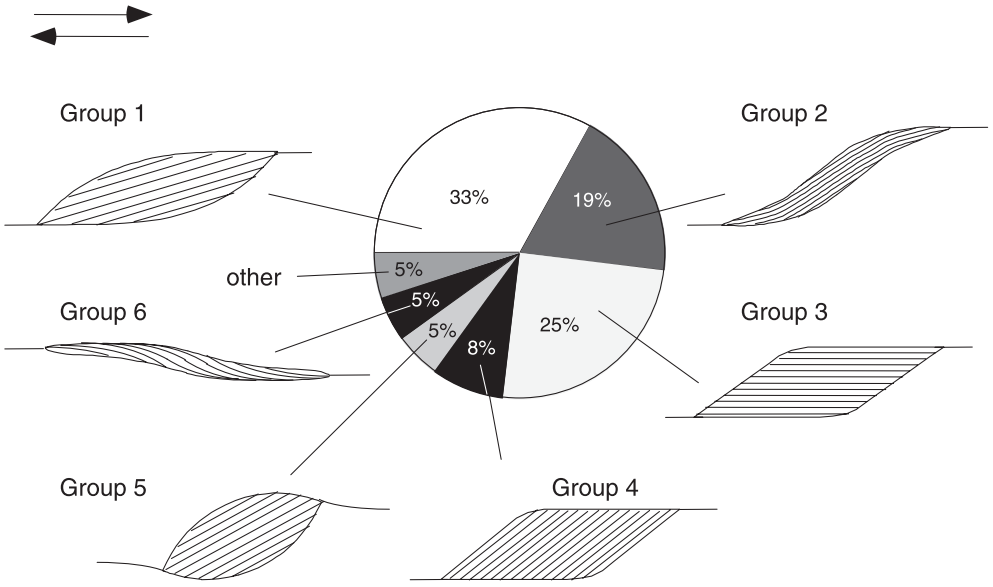

Fig. 4. Schematic drawings of the different morphological types of mica fish. Group 1, lenticular mica fish; group 2, lenticular fish with points inclined in the direction of the foliation; group 3, rhomboidal shaped fish with (001) parallel to longest side of the fish; group 4, rhomboidal shaped fish with (001) parallel to the shortest side of the fish; group 5, fish with small aspect ratio and curved tails; group 6, mica fish with high aspect ratio and inverted stair stepping; if considered out of their context, these structures could lead to an erroneous shear sense determination.

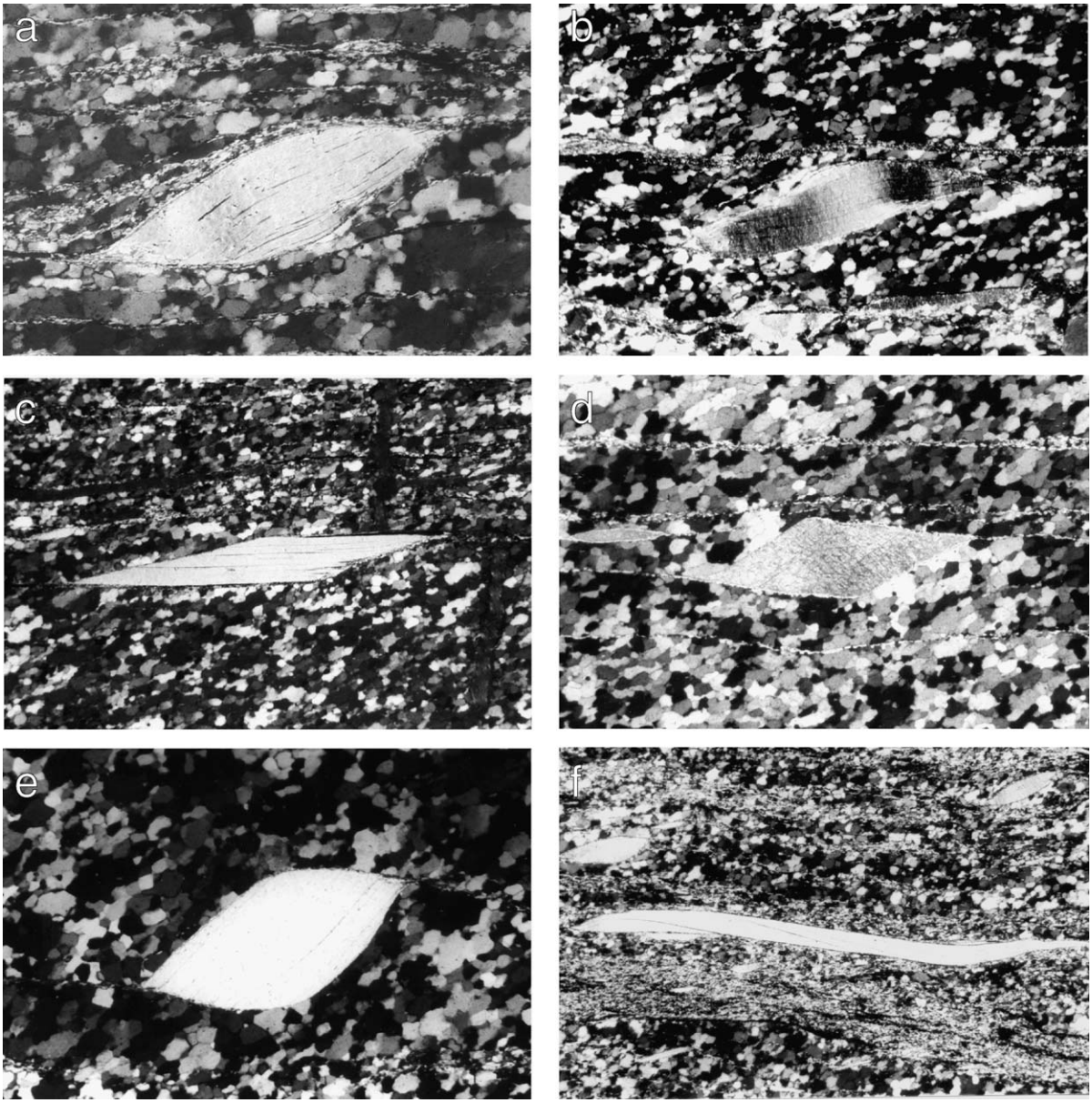

Fig. 5. Photomicrographs of different types of mica fish. (a) Lenticular fish, group 1; (b) lenticular mica fish with slightly inclined tips showing undulose extinction, group 2; (c) rhomboidal shaped fish with (001) parallel to longest side of the fish, group 3; (d) rhomboidal shaped fish with (001) parallel to the shortest side of the fish, group 4; (e) fish with small aspect ratio, group 5; (f) mica fish with high aspect ratio belonging to group 6. Samples are from Conceição do Rio Verde, Brazil. Shear sense in all photographs is dextral. Width of view (a) 3 mm, (b) 0.75 mm, (c), (d) and (e) 3 mm, (f) 6 mm. Crossed polars.

the mica fish, is characterised by thick lens shapes (Figs. 4 and 5e). The orientation of the lattice planes is not clearly related to the long axes of the fish in this group (Fig. 3c). The sides of the mica fish of this type are typically smoothly curved. The difference between this group and the previous groups is that the trails of fine-grained mica are not on the same line as the upper and lower parts of the central mica fish, but curved

towards the points (Fig. 4). The last group, group 6, representing 5% of the studied mica fish, consists of elongate thin micas. The average aspect ratio of mica fish belonging to this group is 9.7. They are usually orientated with their long axes parallel or at a small antithetic or synthetic angle to the mylonitic foliation, and sometimes also a slight stair-stepping of the mica trails in the opposite direction as compared to the mica fish of other groups. Therefore, these thin micas, if considered separately, could lead to an erroneous shear sense determination (Figs. 4 and 5f). Lattice planes usually make a small synthetic angle (Fig. 3c). Most of the mica fish can be placed in one of these groups, but transitions between the different shapes are also observed and some fish shapes (about 5%) do not fit in any of the groups. This subdivision does not depend on the grain size of the mica, small and large mica fish are distributed equally over the different groups. The different groups are equally represented across the entire shear zone and do not depend on local variations in the matrix composition.

3. Evolution of mica fish

The mica fish presented in paper are porphyroclasts and, as such, are derived from pre-existing grains by some deformation mechanism. Lister and Snoke (1984) consider that mica fish are produced by boudinage and microfaulting of pre-existing mica grains, but as they point out, certainly more mechanisms are involved. We consider the main relevant mechanisms: (1) internal deformation, especially slip on (001) basal planes; (2) rigid body rotation; (3) bending and folding of mica grains; (4) grain size reduction either by dynamic recrystallisation at the rims or by cataclastic behaviour resulting in the detachment of small fragments; and (5) pressure solution or diffusional mass transfer, possibly accompanied by local growth. The role of each of these is evaluated below.

(1) Mares and Kronenberg (1993) carried out experiments on shortening of single mica grains. They have shown that due to their mechanical anisotropy, muscovite single crystals deform by several mechanisms depending on the orientation of the cleavage planes. In their experiments the deformation was either accomplished by dislocation glide, where the crystals were shortened at 45° to (001), by kinkbands where shortening was parallel to (001) or by fracturing where the crystals were shortened at 90° to (001). Slip on (001) by dislocation glide is clearly an important deformation mechanism in muscovite, but the effect of this mechanism depends on the orientation of the cleavage planes with respect to the shortening direction and on the critical resolved shear stress necessary to initiate deformation by this mechanism. In non-coaxial flow, the sense of movement can be antithetic or synthetic. This phenomenon has been described for grains with a single slip system (e.g. Echecopar, 1977; Ishii and Sawaguchi, 2002) and for grains transected by microfaults (Simpson and Schmid, 1983; Passchier and Trouw, 1996) and probably works in the same way for slip on (001) in mica crystals.

Ishii and Sawaguchi (2002) investigated the relationship between grain shape and lattice orientation, assuming crystal-plastic deformation by dislocation glide on a single slip system, with a geometrical two-dimensional model. Their study shows the relation between aspect ratio, angle between glide plane and flow plane, and angle between the longest dimension of the clasts and the flow plane. Objects with a glide plane orientation between 30° and 40° are hardly deforming internally, depending also on the aspect ratio of the object. With an orientation of the glide planes between −20° and 30° glide is usually synthetic and for other orientations antithetic. Ishii and Sawaguchi (2002) assume that the grain has the same ductility as the matrix, which is probably not the case for mica fish.

In mica fish with cleavage planes parallel to the mylonitic foliation (group 3; Fig. 4), or at a small synthetic angle (group 6; Fig. 4), slip on (001) is synthetic. For mica fish that lie with cleavage planes at a significant antithetic angle to the foliation (groups 1, 2 and 4; Fig. 4), this mechanism will probably have only minor influence on further modification of the shape because the critical resolved shear stress is not likely to be exceeded. The relative importance of this mechanism is therefore directly related to the orientation of potential slip planes with respect to the flow plane. For the different groups defined above this would mean that the mica fish of groups 3 and 6 have a favourable orientation for this mechanism to have played an important role in the achievement of their present shape. However, as argued in the next paragraph, many mica fish apparently rotated with respect to the flow direction during the early stages of the deformation to

achieve a stable position, so internal deformation may have played an important role during progressive rotation of micas of the other groups as well.

(2) The relative importance of rigid body rotation can be estimated from the preferred shape orientation. All mica fish are orientated with their long axes between $-8°$ and $32°$ with the mylonitic foliation (Fig. 3a; in this study antithetic or back-tilted angles with respect to the main mylonitic foliation are considered positive and synthetic angles negative). This shape-preferred orientation indicates that a stable or semi-stable position was reached in the early stages of the progressive non-coaxial flow. Similar orientations were reported for mica fish from other localities (Eisbacher, 1970; Lister and Snoke, 1984), and for fish-shaped elongated porphyroclasts of other mineral species (Pennacchioni et al., 2001; Mancktelow et al., 2002). Analytical studies of rotating elliptical rigid objects in a homogeneous Newtonian viscous matrix do not predict a stable position for particles in progressive simple shear (Jeffery, 1922; Ghosh and Ramberg, 1976). Masuda et al. (1995) studied distribution patterns of the long axes of initially randomly distributed elliptical particles in general plane strain flow according to the equations given by Ghosh and Ramberg (1976). These patterns show that in simple shear there is a concentration of the orientation of the long axes, depending on the amount of strain. However, none of the patterns given for simple shear or combinations of pure and simple shear as given by Masuda et al. (1995) is similar to the distribution pattern of the measured mica fish.

The experimental results by ten Grotenhuis et al. (2002) and Mancktelow et al. (2002) show that flow in rocks with developing "fish" is probably highly partitioned, i.e. strain is concentrated along micro-shear zones (ten Grotenhuis et al., 2002) or strain is localisation around the objects (Mancktelow et al., 2002) This strain localization causes rigid particles to attain stable antithetic positions consistent with those that were measured. Particles rotate backward if they are initially sub-parallel to the foliation or forward if they are initially oriented at a high angle to the foliation, to attain their stable orientation.

In thin sections of an upper greenschist facies mylonitic quartzite from a location between Cristina and Pedralva, southern Minas Gerais, Brazil (0498972E/7574231N) with 25–30 vol.% mica, such micro-shear zones are indeed abundant (Fig. 6). Lister and Snoke (1984) also show such textural evidence of micro-shear zones along upper and lower limits of mica fish, that extend into the matrix (their Figs. 3b,d, 4, 7, 9a,c and 17a,b). Indeed, the main reason why Lister and Snoke (1984) classified mica fish bearing mylonitised quartzites as S–C mylonites is precisely the presence of C-surfaces, defined as surfaces related to localised high shear strains. This can be considered as textural evidence supporting a mechanism comparable to the ones simulated in the experiments by ten Grotenhuis et al. (2002) and Mancktelow et al. (2002). However, in the samples from Conceição do Rio Verde (Fig. 5) with a low mica content and isolated mica fish in the quartz matrix dynamic recrystallisation of quartz is strong, as indicated by the well-developed oblique quartz fabric, and micro-shear zones may have been erased by the recrystallisation. The lack of evidence for micro-shear zones in many mylonite samples with mica fish is therefore probably an effect of strong dynamic recrystallisation favoured by a low percentage of mica. In contrast, the presence of abundant trails of fine-grained mica definitely restricts grain growth of quartz in the matrix, promoting the preservation of evidence for micro-shear zones in samples with a high percentage of mica.

(3) The importance of bending and folding of mica fish (Lister and Snoke, 1984, their Fig. 5i,j) can be judged from their common undulatory extinction (Fig. 5b). One out of five mica fish belongs to group 2 with bent tips (Fig. 4). Kink folds were observed in some mica fish with their lattice planes orientated sub-

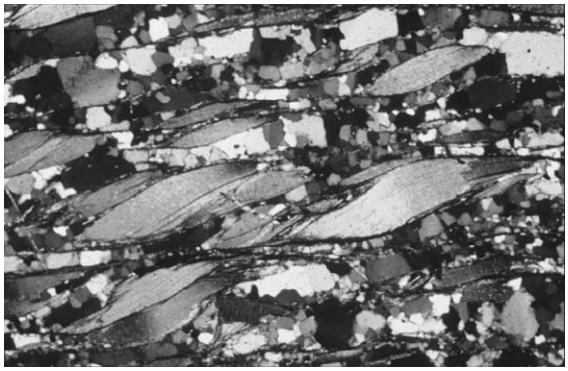

Fig. 6. Photomicrograph of mylonitic quartzite with mica fish and micro shear zones. Sample courtesy Rodrigo Peternel. Varginha, Minas Gerais, Brazil. Width of view 4 mm. Crossed polars.

parallel to the mylonitic foliation (Fig. 7a). These structures indicative of shortening are probably generated when the basal planes of parts of the fish rotate into the shortening quadrant of the flow. Mica fish with isoclinally folded tips are relatively common (ca. 5%, Fig. 7b).

(4) The importance of grain size reduction can be estimated from the large number of small mica grains that are formed, either by dynamic recrystallisation or by cataclasis at the sides and tips of the mica fish (Fig. 5). Recrystallisation of muscovite may result from rotation of small parts at the boundary of the fish. Growth of these parts would produce small new mica grains (Lister and Snoke, 1984). These new grains are subsequently torn into the matrix by intense ductile deformation to form the trails that define the mylonitic foliation. The amount of small apparently recrystallised grains is high at the sides of the mica fish that make a significant angle with the (001) planes (Fig. 5c) indicating that this grain size reduction mechanism is most intense at these sides. This mechanism can also contribute to the development of the fish shape of the mica grains by rounding the corners of the crystals. According to Lister and Snoke (1984) the convergence of lattice planes on a discontinuity in the tips of some mica fish (Figs. 4 and 5b) is also due to a recrystallisation mechanism. They suggest that rotation of the cleavage planes towards parallelism with the boundary followed by migration recrystallisation leads to the formation of a recrystallisation front, which is observed as a discontinuity in the crystal. An attempt was made to detect possible cut-off effects by erosion of zoned grains with the help of microprobe analysis. However, all analysed mica fish proved extremely homogeneous in composition, not showing any zoning pattern.

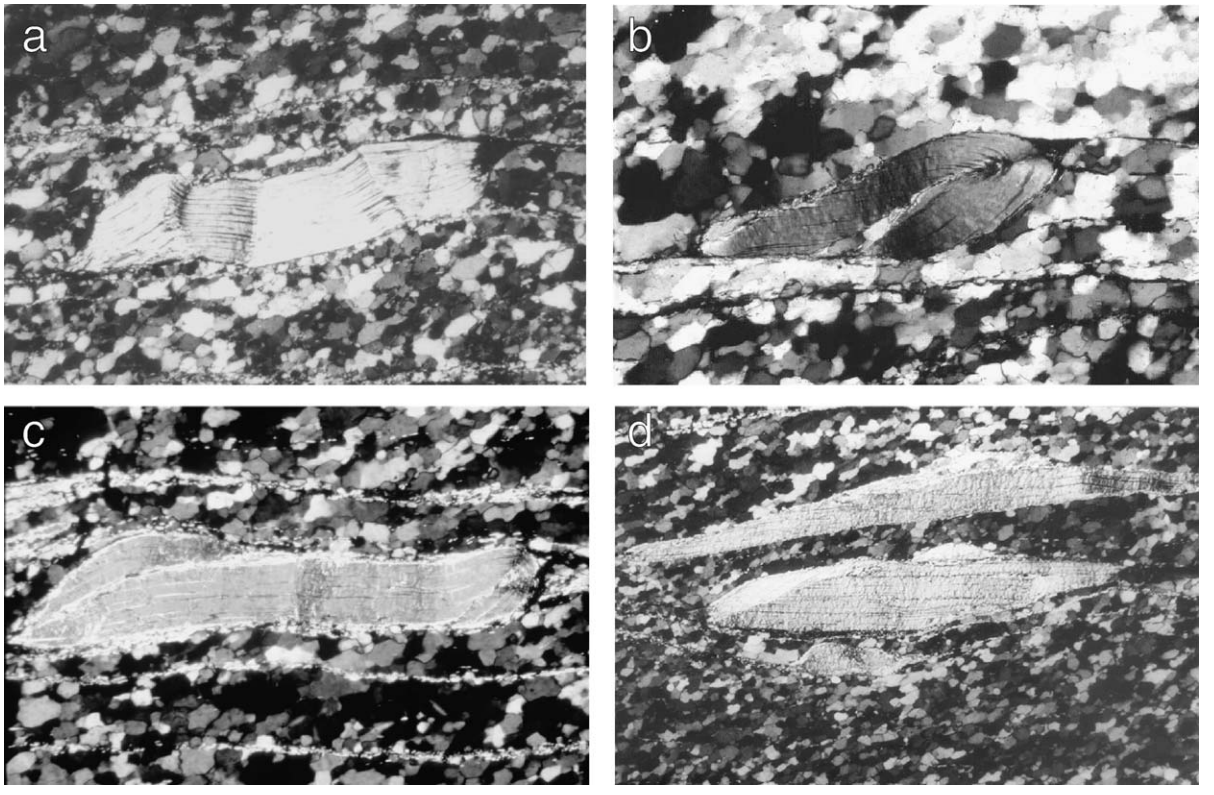

Fig. 7. Photographs showing different types of folds in mica fish. (a) Kinkfolds. (b) Isoclinal fold. (c) Folded mica fish with tight fold hinges, on the left side the fish is separated in two parts along the fold hinge. (d) On top of the lower mica fish is a small mica grain, which can be interpreted as a fragment broken off from the tip and now being transported along the grain. Samples are from Conceição do Rio Verde, Brazil. Shear sense is dextral and width of view 3 mm in all photographs. Crossed polars.

Apart from the one-to-one formation of mica fish from isolated crystals in the protolith there is also microstructural evidence for mechanisms where one large crystal is divided into several smaller ones. Lister and Snoke (1984) drew attention to several microstructures related to the peeling off of smaller fish from large ones. They proposed a model of boudinage related to the fact that the majority of the mica fish lie with their long axes in the extensional quadrant of the deformation and have a lens or barrel shape that resembles boudins. Direct evidence of boudinage in the form of two pieces that can be linked together is locally present in our studied material, but is uncommon. We therefore consider this process to be of secondary importance. An alternative mechanism for the peeling off of smaller mica fish is demonstrated in Fig. 8. In this process, the tips of the fish are folded and separated from the parent crystal along tightly bent fold hinges, approximately following the axial plane. The small separated part is subsequently transported over the larger part. Structures that can be interpreted to represent several stages of this process occur with considerable frequency in our studied material (Fig. 7b–d; compare also Lister and Snoke, 1984, their Fig. 7d). Another mechanism to split a mica fish in two parts presented by Lister and Snoke (1984) is the development of fractures parallel to the basal plane of mica (Fig. 9). This process is similar to the earlier described slip along mineral cleavage planes, except that brittle behaviour now results in movement along a fracture, producing seperate crystal fragments. Depending on the orienta-

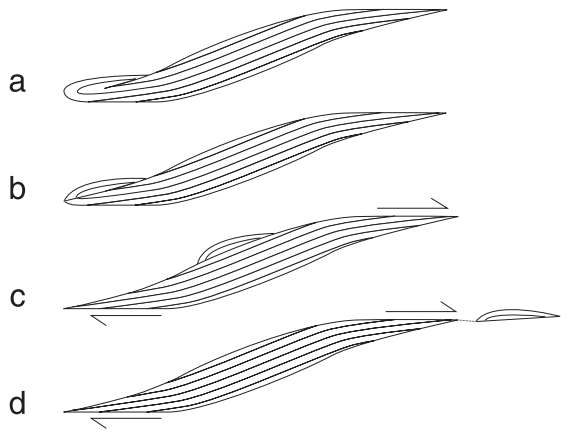

Fig. 8. Schematic drawing of mica fish illustrating a proposed process in which a crystal is divided into two parts. (a) The point of the crystal is folded; (b) the fold becomes very tight and the fish breaks apart along the fold hinge; (c) the smaller part is transported along the side of the bigger part; (d) two separate mica fish have formed.

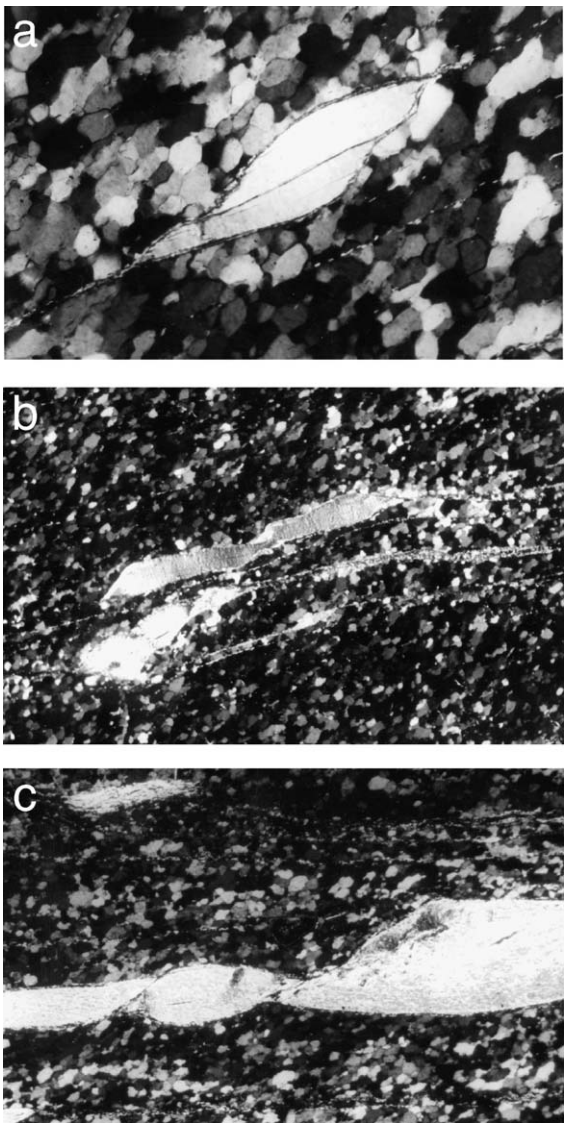

Fig. 9. Photographs of microfaults separating mica fish in two or more smaller parts. (a and b) Different stages of a process in which a mica fish is divided in two parts along basal planes with synthetic sense of movement. (c) Micro-faults through a mica fish at a high angle to the basal planes, showing antithetic movement. All samples are from Conceição do Rio Verde, Brazil. Shear sense in all photographs is dextral. Width of view (a) 1.5 mm, (b) 6 mm, (c) 3 mm. Crossed polars.

tion of the cleavage planes in the mica grains this may result in antithetic or synthetic micro-faults. Evidence for this mechanism is commonly observed in our material, especially for synthetic microfaults in fish with basal planes subparallel to the mylonitic foliation (Fig. 9). Microfaults through the mica fish both at low and high angles to the basal planes were also occasionally observed, showing synthetic or antithetic movement depending on the orientation of the fault (Fig. 9c). Evidence for a mechanism explained by Lister and Snoke (1984) where a smaller fish is separated from his parent by an antithetic listric fault (their Figs. 5g and 6) was not observed in our material.

(5) Pressure solution is a likely mechanism for the development of the rounded shape of mica fish.

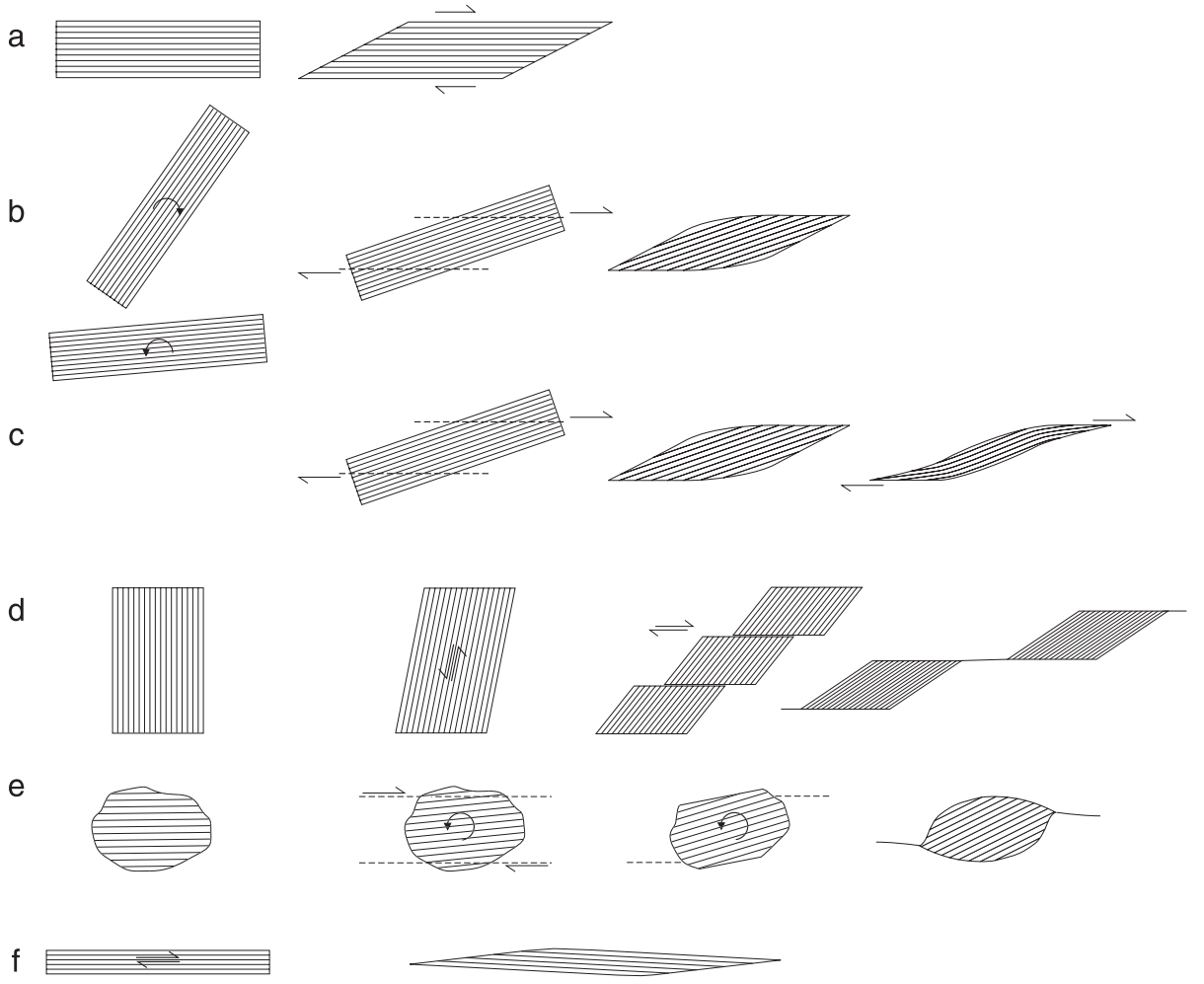

Fig. 10. Explanatory cartoons to show how the different groups of mica fish may have formed. The development is shown in stages to illustrate the processes involved, but these processes are envisaged to act simultaneously in nature. (a) Undeformed mica grain is sheared to group 3 mica fish by slip on (001); (b) a grain is simultaneously rotated and reduced on the upper and lower side as explained in the text, to form a group 1 mica fish; (c) a group 1 mica fish is transformed into a group 2 one by drag along micro shear zones; (d) an undeformed mica grain with its (001) cleavage at a high angle to the foliation may be transformed to a group 4 mica fish by a combination of antithetic slip on (001) planes and separation in several parts along micro shear zones; (e) an irregular shaped mica may be modified to a group 5 mica fish by a combination of rotation and reduction of grain size related to micro shear zones deflecting around the fish; (f) a thin elongate mica grain deformed into a group 6 mica fish by slip on (001).

Experiments by Niemeijer and Spiers (2002) on quartz-mica aggregates have shown a decrease in pressure solution rates for quartz when muscovite is present. They suggested that this is due to Al^{3+} from dissolved muscovite lowering the solubility of quartz. This would mean that pressure solution of muscovite is possible in quartz-mica aggregates. Unfortunately, it is very difficult to find evidence for this mechanism, mainly because the white micas in our samples are not chemically zoned. Pressure solution and solution transfer does play a role in the development of some other fish-shaped mineral grains, as shown below.

Based on the considerations outlined above the following evolution for the different morphological groups is proposed, starting from initially approximately rectangular mica grains as found in the metasedimentary rocks outside the shear zone. From this starting position, the shape of mica fish of group 3 can easily be attained by slip on (001) (Fig. 10a). Micas of groups 1 and 2 probably attained their inclined position by rotation into a stable position (Fig. 10b). The rotation direction of the mica depends on the initial orientation. Pennacchioni et al. (2001) suggested a similar mechanism to explain the shape and orientation of sillimanite porphyroclasts. Experiments by ten Grotenhuis et al. (2002) and Mancktelow et al. (2002) have shown that fish-shaped clasts with an initial orientation parallel to the shear plane can rotate backwards against the shear sense and obtain a antithetic stable position either if matrix flow is partitioned into micro-shear zones or if the clast is decoupled from the matrix. The typical lens shape of group 1 (Fig. 10b) could be explained by the removal of small grains by recrystallisation or fracture along the upper and lower parts, accompanied by pressure solution and/or diffusive mass transfer. The shape of group 2 fish (Fig. 10c) is thought to evolve from group 1 by drag along zones of concentrated shear localised along the upper and lower contacts, comparable to the deflection of S-planes in S–C cleavage (e.g. Passchier and Simpson, 1986).

Mica fish of group 4 could form by antithetic slip on (001) from grains with an original high angle between internal cleavage and foliation (Fig. 10d). The initial grain is probably a fragment of normal-shaped micas orientated at a high angle to the shear zone, which were cut by micro-shear zones into elongate segments, and which then developed into group 4 shapes (Fig. 10d). Group 5 mica fish could be explained as originated from short stubby micas modified by removal of material along curved shear bands in combination with rotation (Fig. 10e). Finally group 6 micas are thought to result from synthetic slip on (001) (Fig. 10f). The (001) planes of the micas in this group are in the right orientation for synthetic slip (Ishii and Sawaguchi, 2002).

In general, the characteristic oblique orientation of mica fish mainly results from rigid body rotation of originally platy mica crystals in the early stages of non-coaxial deformation, reaching a stable position by a mechanism involving localisation in the matrix around the porphyroclast by micro-shear zones. The rotation is accompanied by slip on basal lattice planes, some bending and folding, and 'tectonic erosion' along the rims mainly due to recrystallisation, cataclasis and possibly pressure solution and/or diffusional mass transfer. No evidence indicating grain growth during the process was observed.

4. Porphyroclasts of other minerals with fish shapes

4.1. Previous work

Porphyroclasts with a characteristic fish-shape and shape-preferred orientation are also found in a number of other minerals. Leucoxene fish (Oliver and Goodge, 1996) are developed as alteration products of detrital rutile, ilmenite or titanite in a siliciclastic protolith. Deformation of the initially equidimensional aggregates, as passive bodies in a quartz matrix, results in ellipsoids whose long axes rotated towards the mylonitic foliation with increasing strain. Pennacchioni et al. (2001) determined the shape-preferred orientation of sillimanite, garnet and plagioclase porphyroclasts in an amphibolite facies mylonite from Mont Mary in the Italian western Alps. Their measured porphyroclasts approach a rhomboidal (sillimanite) or elliptical (garnet, plagioclase, sillimanite) shape, with aspect ratios varying between 1 and 11. The long axes of the best-fit ellipses define a very strong shape-preferred orientation, inclined antithetically 5–10°, comparable to the mica fish of this study. They conclude that for rhomboidal sillimanite por-

phyroclasts with aspect ratios higher than three a stable position is acquired. The rhombohedral shape and the inclination of these porphyroclasts are explained by an initial rotation (or back-rotation) of rectangular microboudins towards a stable position inclined to the mylonitic foliation. They would then change their shape to a rhombohedral form by dissolution and/or reaction against extensional crenulation cleavage planes. The orientation data presented by Mancktelow et al. (2002) for porphyroclasts of hornblende, clinopyroxene and rare garnet in a mylonitised metagabbro, for olivine porphyroclasts in an ultramafic mylonite and for elongate sillimanite in pelitic mylonites, confirm the data presented by Pennacchioni et al. (2001) and by ten Grotenhuis et al. (2002) in the sense that they also found very strong shape-preferred orientations at a small antithetic angle (5–10°) to the shear direction for porphyroclasts with aspect ratios higher then 3.

In the material studied for this paper, oblique asymmetric elongated porphyroclasts, similar to mica fish, are also developed in biotite, tourmaline, K-feldspar, garnet, hypersthene, quartz, plagioclase (Fig. 11a), staurolite, kyanite, amphibole, diopside (Fig. 11b), apatite, rutile, hematite and prehnite, in mylonites from a variety of locations and metamorphic grade. This means that they may form in any mineral species capable of forming resistant porphyroclasts in a mylonite. The most significant characteristics of biotite, tourmaline, K-feldspar, garnet, hypersthene and quartz porphyroclasts observed in our study are described below and compared to that of muscovite fish.

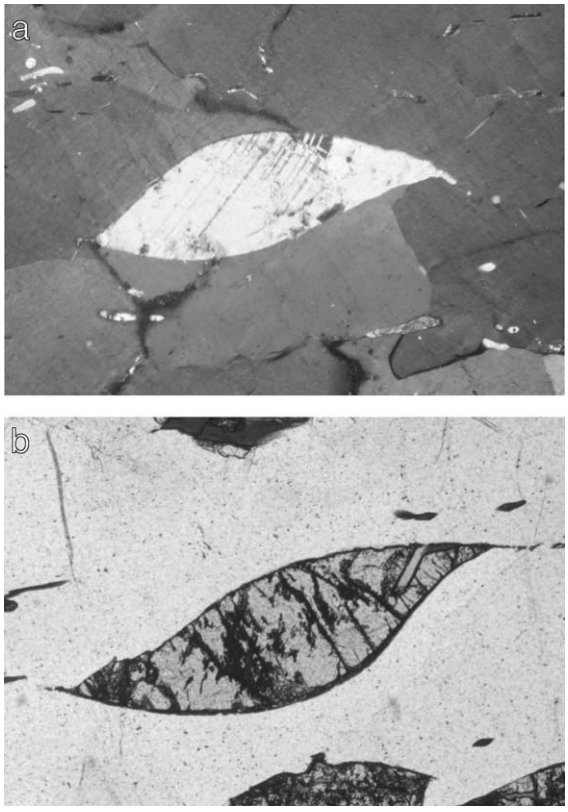

Fig. 11. (a) Photomicrograph of fish shaped porphyroclast of plagioclase surrounded by a recrystallised quartz matrix from a high grade mylonitic gneiss, Morro Cara de Cão, Rio de Janeiro, Brazil. Width of view 2 mm, crossed polars. (b) Photomicrograph of fish shaped porphyroclast of diopside surrounded by a recrystallised quartz matrix, from a high grade mylonite, Varginha, Minas Gerais, Brazil. Sample courtesy Rodrigo Peternel. Width of view 2 mm. Parallel polars. Shear sence in both photographs is dextral.

4.2. Biotite

Biotite fish are much less common than muscovite fish. The studied samples are mylonitized granodiorites from the Santa Rosa mylonite zone in Palm canyon at Palm Springs, California. They are rich in quartz and biotite with minor amounts of plagioclase, K-feldspar and muscovite. The muscovite in these samples also shows fish-shapes. The samples are deformed under middle amphibolite facies conditions (Wenk and Pannetier, 1990; Goodwin and Wenk, 1995). The biotite and muscovite fish from this location are lenticular in cross-sections parallel to the stretching lineation and perpendicular to the foliation (Fig. 12a), similar to the muscovite fish described above (Fig. 4). Measurements of the angle between the long axes of 69 biotite fish and the mylonitic foliation gave a mean value of 12° (Fig. 13a) and measurements of 31 muscovite fish produced a similar angle of 15°. Both angles are very close to the mean angle for muscovite fish from Minas Gerais. Their morphology, similar to that of group 1 of the muscovite fish, suggests that biotite fish are essentially formed by the same mechanisms as suggested above for the group 1 muscovite fish, mainly a combination of rotation and recrystallisation. Compared to muscovite, biotite is more resistant to slip on (001) (Mares and Kronenberg, 1993), but the recrys-

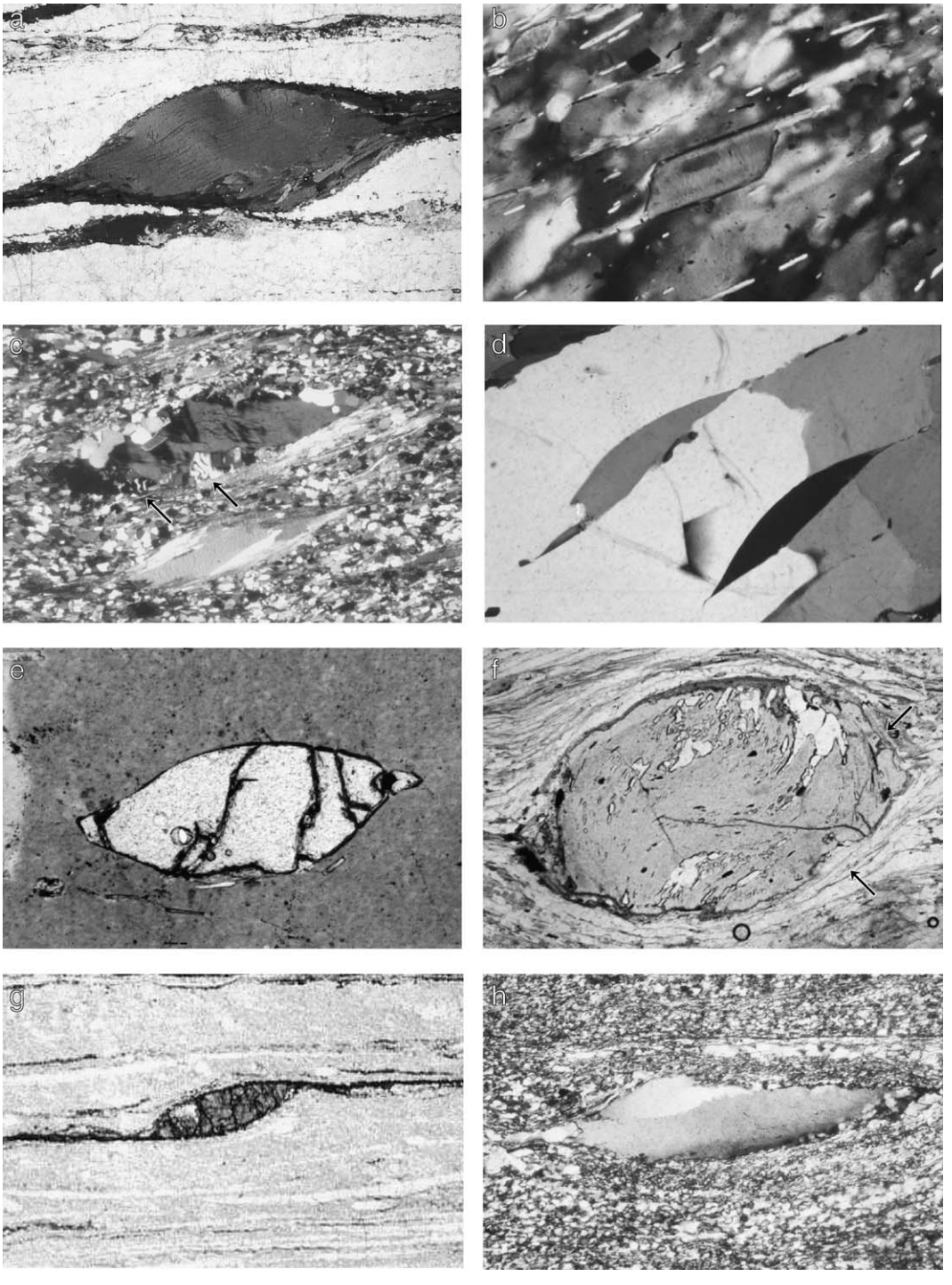
a
b
c
d
e
f
g
h

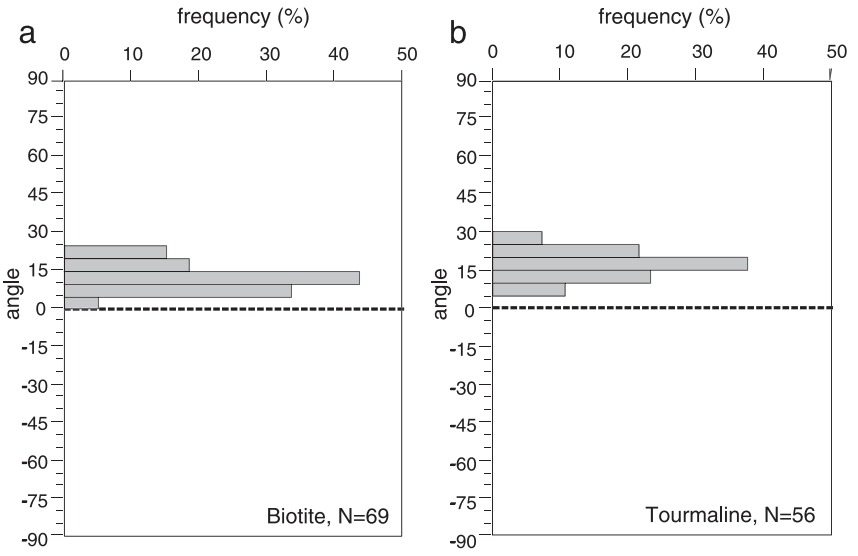

Fig. 13. Orientation of the long axes with respect to the mylonitic foliation of (a) 69 biotite fish from the Santa Rosa mylonite zone, California and (b) 56 tourmaline fish from Lambari, Minas Gerais, Brazil.

tallisation mechanism is essentially the same. Rotation of part of the crystals may lead to high angle boundaries and formation of new grains (Etheridge and Hobbs, 1974). In the studied thin sections, the muscovite fish are surrounded by very small amounts of recrystallised material, whereas the biotite fish are surrounded by a much thicker mantle of recrystallised material (Fig. 12a). Under similar conditions, it therefore seems that biotite recrystallises more readily than muscovite (Passchier, 1985). This increased tendency to recrystallise may account for the less frequent occurrence of biotite fish in nature, as compared to muscovite fish.

4.3. Tourmaline

The studied tourmaline porphyroclasts come from a mylonitic quartzite derived from a sedimentary protolith of the Andrelândia Depositional Sequence (Paciullo et al., 1993; Ribeiro et al., 1995), near Lambari, Minas Gerais, Brazil (0457716E/7566341N). The estimated metamorphic grade during deformation of these samples is lower to middle amphibolite facies. The tourmaline crystals usually have a rhomboid shape with straight sides and typically an angle of about 50–55° between the sides (Fig. 12b). The tourmaline crystals have a strong shape-preferred orientation. The angles between the long axes of 56 tourmaline porphyroclasts and the mylonitic foliation gave a mean value of 16° (Fig. 13b), similar to the mean value for the measured muscovite and biotite fish. The shape-preferred orientation is a result of rotation of the crystals, similar as described for the mica fish. Their shape is very similar to the mica fish of groups 3 and 4, a parallelogram shape with the long side parallel to the mylonitic foliation.

Fig. 12. Photomicrographs of different minerals showing fish shapes similar to mica fish. (a) Biotite fish with small recrystallised biotite grains along the rims, from Santa Rosa Mylonite zone, California. (b) Tourmaline fish showing rhomboidal shape from Lambari, Brazil. Crossed polars. (c) K-feldspar fish with subgrains along the rim, Roraima, Brazil. Myrmekite along the rim is indicated by the arrows. Crossed polars. (d) Elongate monocrystalline K-feldspar fish in a recrystallised quartz matrix. Crossed polars. (e) Garnet fish in static recrystallised quartz matrix, Morro Cara de Cão, Brazil. (f) Garnet fish in quartz-mica matrix with chlorite concentrated along upper and lower rims, Santana do Garambeu, Brazil. Note the straight crystal faces preserved at the right-hand side of the garnet crystal and chlorite at the long sides of the crystal (arrows). (g) Hypersthene fish with trails of recrystallised material, Caparao, Brazil. (h) Quartz fish in fine-grained matrix composed of quartz and mica with elongated subgrains, Serra do Espinhaço, Brazil. Crossed polars. Shear sense in all photographs is dextral. Width of view (a) 6 mm, (b) 1.5 mm, (c) 1.5 mm, (d) 2 mm, (e) 1.5 mm, (f, g and h) 3 mm.

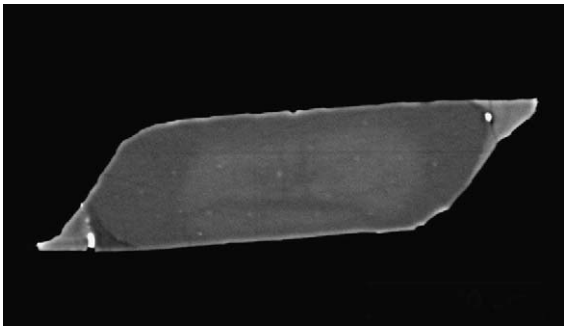

Fig. 14. BSE image of tourmaline fish from Lambari, Brazil, showing zoning in the centre and new growth of tourmaline at the tips of the fish. Width of view 140 μm.

The studied tourmaline porphyroclasts do not show evidence for internal deformation. Back-scatter electron (BSE) images of the tourmalines show brighter newly grown tips (Fig. 14) and zoning, which is often cut-off at the edges in the shortening quadrants of the flow. This suggests that the shape of the tourmaline porphyroclasts is the result of dissolution or diffusional mass transfer along the edges in the shortening quarters of the fish and grain growth by precipitation or by diffusional mass transfer at the tips.

4.4. K-feldspar

Lenticular shaped K-feldspar porphyroclasts have been described by Simpson and Wintch (1989) from an S–C mylonite. The tips of these K-feldspar grains are recrystallised and quartz-plagioclase symplectite (myrmekite) is developed in shortening quarters in the rims of the crystals. The reaction from K-feldspar to plagioclase and quartz is favoured at sites of high normal stress, because it involves a volume decrease (Simpson and Wintch, 1989). Fish-shaped K-feldspar porphyroclasts used in this study come from the Espinhaço Belt, Diamantina, Minas Gerais, Brazil, from Roraima, northern Brazil, and from Varginha, Minas Gerais, Brazil. The studied samples are deformed under upper greenschist facies (Espinhaço Belt), lower amphibolite facies (Roraima), and upper amphibolite to granulite facies conditions (Varginha). The K-feldspars from the first two localities usually have a disc shape and a shape-preferred orientation with the longest dimension at a small antithetic angle to the main mylonitic foliation. Subgrains and recrystallised new grains are concentrated in the rim of the porphyroclast (Fig. 12c). Concentration of mica at the sides of the clasts suggests that pressure solution and/or retrograde reactions played a role in the development of these porphyroclasts. In the samples from the Espinhaço Belt, the K-feldspar fish have myrmekite along their rims, in the shortening quadrants of the flow (Fig. 12c). Apparently, the mechanisms that contributed to the formation of lower temperature K-feldspar fish are principally recovery and recrystallisation along the rims, resulting in a softer mantle that is asymmetrically deformed to a sigma structure (Passchier and Simpson, 1986). This process was probably accompanied by rigid body rotation and in some cases myrmekite formation. Internal deformation by dislocation glide is certainly less important than in muscovite at this metamorphic grade, but dissolution or transformation into other mineral species by retrograde metamorphic reactions may have been more significant. The higher grade sample from Varginha shows highly elongated monomineralic K-feldspar fish (Fig. 12d) with a strong SPO and some undulose extinction. They are surrounded by large recrystallised quartz grains. Gower and Simpson (1992) concluded that phase boundary cusps in the direction of the foliation in high-grade quartzofeldspatic rocks cannot be formed by dislocation creep alone, but also involve a diffusion-assisted process with dissolution at foliation parallel phase boundaries and precipitation in the cusps. These cusps are similar to what we have called here the tips of the fish. The combination of the undulose extinction in the K-feldspar from Varginha, and the sharp tips or cusps of these fish suggests deformation by both dislocation and diffusional creep. In general terms the formation of K-feldspar fish seems to need higher metamorphic grade than muscovite fish, since both the minimum temperature for recrystallisation and for crystal-plastic behaviour are considerably higher (e.g. Tullis and Yund, 1991).

4.5. Garnet

Fish-shaped garnets from a middle amphibolite facies shear zone were reported by Azor et al. (1997). Compositional X-ray maps of their samples

show that the growth zoning is truncated along the borders of the garnets. Based on this fact, they claim selective dissolution as the main mechanism responsible for the final shape of the garnets in their samples. Ji and Martignole (1994) studied elongated garnets in high-grade rocks and suggested dislocation slip and recovery as deformation mechanisms for their garnets, although Den Brok and Kruhl (1996) argued that these structures could also have formed by grain boundary diffusional creep. The fish-shaped garnet porphyroclasts reported here are from two high-grade, mylonitised pelitic metasediments, a granulite facies mylonite from Varginha, Minas Gerais, Brazil (0461750E/7616252N), and a high amphibolite-granulite facies mylonite from Morro Cara de Cão, Rio de Janeiro, Brazil (Fig. 12e). A third set of samples with garnet porphyroclasts (Fig. 12f) is from a lower amphibolite facies garnet-staurolite schist from Santana do Garambeu, Minas Gerais, Brazil, with white mica and biotite in the matrix. The garnets from the two high-grade mylonites are mainly surrounded by quartz and have lenticular shapes with pointed tips (Fig. 12e). They have a strong shape-preferred orientation with the long axis at an antithetic angle with respect to the flow direction. The morphology of these garnets suggests that they are probably deformed by diffusion creep or selective dissolution. Since the quartz matrix in these samples is statically recrystallised after mylonitisation, the fish-shape and the shape-preferred orientation of the garnet crystals are the only kinematic indicators in these rocks.

Garnet porphyroclasts from Santana do Garambeu formed under lower amphibolite facies conditions and may initially have had idiomorphic crystal shapes, since in some of these garnets straight crystal faces were found at the sides in the extensional quadrant of the strain ellipsoid (Fig. 12f). The elongate shape and the antithetic orientation of the long axis of these grains is probably the result of a grain size reducing mechanism enhanced at the long sides of the crystals, perpendicular to the principal shortening direction, combined with rigid body rotation of the fish-shaped structure towards the current position. The reduction of the grain size is probably the result of a retrograde reaction, as indicated by the concentration of chlorite along the long sides of the garnet crystals.

4.6. Hypersthene

Fish-shaped hypersthene porphyroclasts were found in a granulite facies quartz-feldspar-rich orthogneiss from a mylonite zone near Caparao, Minas Gerais, Brazil. They have an elongated fish-shape and a strong SPO with small antithetic angle to the mylonitic foliation, with very clear stair stepping of trails of fine-grained material (Fig. 12g). Small fragments of hypersthene are found mainly at the rim surrounding the porphyroclasts and in trails extending from their tips into the matrix, related to micro-shear zones. These fragments suggest cataclastic abrasion or recrystallisation of the crystals. Microprobe analysis established that the hypersthenes are very homogeneous in composition, without any detectable zoning. Crystal-plastic deformation of the porphyroclasts was probably not important, in contrast to orthopyroxene grains in peridotite described by Ishii and Sawaguchi (2002). The strength of the grains and the olivine matrix is nearly equal in their samples. The strength of the quartz-rich matrix (e.g. Hirth et al., 2001) in our samples is estimated to be lower than the strength of the hyperstene grains. The fish shape seems to be essentially developed by rotation of pre-existing grains, accompanied by cataclastic abrasion and possibly recrystallisation and dissolution along the rims of the crystals.

4.7. Quartz

Fish-shaped quartz porphyroclasts are uncommon in mylonitic rocks, since quartz tends to constitute the matrix rather than porphyroclasts in most mylonites. Quartz can only survive as porphyroclasts in a soft and usually fine-grained matrix. Bestmann (1999) and Bestmann et al. (2000) describe the shape of fish-shaped single strain-free detrital quartz grains in a calcite matrix. Lattice diffusion creep is suggested to explain the shape of these grains. Williams and Burr (1994) describe deformed and undeformed quartz phenocrysts from a metarhyolite. The deformed quartz phenocrysts have elliptical cross sections and exhibit undulose extinction, subgrains and irregular boundaries, suggesting internal deformation by lattice slip and dynamic recrystallisation.

The studied quartz fish occur in lower greenschist facies protomylonites of volcanic origin from Serra

do Espinhaço, Minas Gerais, Brazil. The quartz fish are originally quartz phenocrysts embedded in a fine-grained matrix (Vernon, 1986; Williams and Burr, 1994), now consisting of mica and quartz. The elongated quartz grains exhibit undulose extinction and irregular boundaries (Fig. 12h). These elongated grains have a similar shape and shape-preferred orientation to the mica fish of group 2. The microstructures are comparable to the deformed phenocrysts studied by Williams and Burr (1994). The quartz crystals contain highly elongated subgrains and also domains with small recrystallised grains, mainly at the tips of the fish. Some domains of small recrystallised grains are subparallel to the long axes of the fish-like bodies, separating them into two parts in a similar way to the microfaults in the white mica fish (Fig. 9). The combination of large subgrains and domains of small recrystallised grains is a fabric typical of dynamic recrystallisation due to internal deformation in quartz. Recrystallisation at the tips of the fish tends to destroy the fish shape. The concentration of mica on the sides perpendicular to the shortening direction indicates that pressure solution also played a role in the formation of the fish shape. It can be concluded that these fish-like quartz crystals were essentially formed by crystal-plastic deformation.

5. Discussion and conclusions

Investigation of the morphology of mica fish led to a subdivision into six groups. Although evolution of fish from one group into another is possible, most of these groups are thought to represent stable or semi-stable structures. The evolution of each group is thought to initiate with a combination of rigid body rotation and crystal-plastic deformation, essentially by slip on (001). Reduction of the grain size along the upper and lower part of mica grains mainly by recrystallisation tend to enhance the fish shape. Contrary to the mechanism that forms sigma-type mantled porphyroclasts (Passchier and Simpson, 1986), this recrystallised material is not accommodated in the strain shadow of a rounded core object, but forms thin trails from the tips of a fish-shaped single crystal (Fig. 1a). This grain size reduction may also be achieved by cataclastic breakdown, by pressure solution or by diffusional mass transfer. These micro-shear zones are usually straight and parallel to each other, but may also deflect around the widest part of the fish to produce a reduced stair stepping effect (Fig. 4, group 5).

Minerals other than white mica can also form similar fish-shaped single crystals but these show considerable variation in original shape, competency contrast with the matrix and amount of crystal-plastic deformation. Biotite behaves similarly to muscovite but recrystallises more readily resulting in less common survival of biotite fish. Tourmaline shows little or no intracrystalline deformation but changes shape by dissolution and precipitation or by diffusional mass transfer. K-feldspar can transform into K-feldspar fish by recrystallisation at the rims of the crystals. At high temperatures, crystal-plastic deformation becomes the most important deformation mechanism. The evolution of fish-shaped garnet crystals is at lower temperatures related to removal of garnet by pressure solution or by reaction. At higher temperatures, crystal-plastic deformation may play an increasingly important role. Hypersthene crystals do not show evidence of internal deformation and, at least in our samples, seem to have formed essentially by grain size reduction mechanisms. Quartz may in rare cases survive as fish-shaped crystals in a fine-grained host rock. It is mainly deformed by strong crystal-plastic deformation and the relatively large fish-shaped crystals tend to disappear mainly due to recrystallisation. The value of these comparisons is obviously only relative since the relative importance of different processes can rarely be quantified and other factors, like metamorphic grade, strain intensity, the presence and composition of fluids and strain rate, were not taken into account. Nevertheless, the shapes and the shape-preferred orientations of the different minerals are very similar, despite a number of salient differences in their development. The shape and the shape-preferred orientation of the mineral fish must be seen as two inseparable aspects of these microstructures. The shape-preferred orientation can only develop due to the specific shape of the crystals. On the other hand, the stable orientation ensures that processes like recrystallisation and dissolution, which are more significant in the shortening quadrants of the flow, influence the same part of the crystal during progressive deformation, thereby enhancing the fish-shape.

Most mineral fish can be used to infer the sense of shear in zones of non-coaxial flow. Their asymmetrical, lenticular or rhomboidal shape and the inclination of their long axes with respect to the mylonitic foliation makes them reliable kinematic indicators, with the exception of group 6 mica fish which, if considered in isolation, would lead to an incorrect interpretation of the sense of shear. Even in samples where the matrix is statically recrystallised, mineral fish retain the asymmetric geometry necessary to correctly deduce the sense of shear (e.g. Fig. 11a,b).

The results of experimental work (ten Grotenhuis et al., 2002; Mancktelow et al., 2002) and our observations have thrown new light on the possible development of shape-preferred orientations. In simple shear flow without partitioning and with perfect cohesion between rigid objects and their matrix, theory predicts that rigid objects with perfect bonding to the matrix should continuously rotate forward with respect to the shear plane and shear sense (Jeffery, 1922).

We suggest that there are two ways in which stable, non-rotational positions with respect to flow axes can be attained by rigid or relatively strong objects in ductile flow (Fig. 15): (1) synthetic for non-partitioned flow around rigid elongate porphyroclasts in non-coaxial general progressive deformation, following the Jeffery (1922) model and (2) antithetic for settings with localised flow close to the porphyroclasts as observed in experiments (ten Grotenhuis et al., 2002; Mancktelow et al., 2002) and in our observations. The synthetic positions can be explained as an effect of balancing forces on parts of the clasts that lie in synthetic and antithetic flowing segments of bulk non-coaxial general flow separated by bulk flow eigenvectors (Fig. 15). A synthetic orientation can only be obtained if there is a pure shear component in the flow and the aspect ratio of the rigid object is not to small (Ghosh and Ramberg, 1976). The antithetic positions cannot be explained in this way, but can be understood if one considers the effect of micro-shear zones suitably placed in a partitioned flow. Flow on micro-shear zones nucleated from the tips of a lens-shaped porphyroclast that would generate a couple of extensional and compressional forces in the matrix material on the sides of the fish. These forces are tending to rotate them in a counter clock-wise sense for a bulk dextral shear sense (Fig. 15). Since the general non-coaxial flow in the matrix tends to rotate the fish in a clockwise sense both forces counteract each other and could therefore maintain the fish in a stable position. Mechanical erosion, pressure solution and internal deformation could subsequently give the fish its characteristic shape.

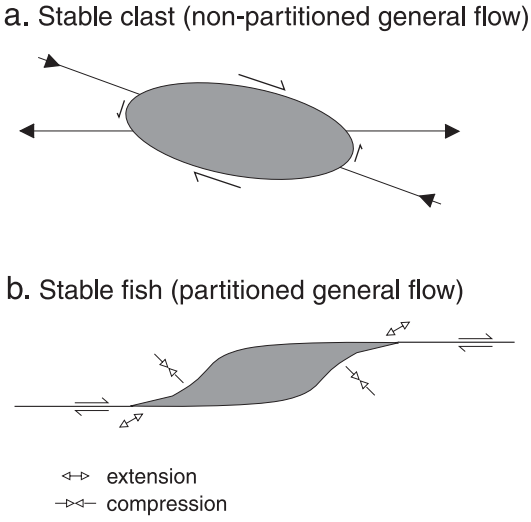

Fig. 15. Sketch to show (a) the effect of balancing forces on parts of a clast that lies in synthetic and antithetic flowing segments of bulk non-coaxial flow, and (b) how the presence of minor shear zones along tips of mineral fish may produce a couple of forces that act in a counter clockwise sense, to balance the tendency for clockwise rotation induced by the general flow of the matrix.

The ideas presented here and by Lister and Snoke (1984) regarding the separation of parts of mica fish are based on inhomogeneous flow around these structures. The proposed transport of separated parts of the fish along the grain boundary of the host clast is only possible if there is a micro-shear zone along this boundary (Fig. 15). It is also possible to transport relatively small recrystallised fragments of the fish far into the matrix along such micro-shear zones, as observed for muscovite, biotite and hypersthene. The observed orientation distributions for muscovite, biotite and tourmaline fish also imply that flow is partitioned into narrow shear zones. The fabric of mica fish, with trails of fine-grained mica extending from the tips of the fish into the matrix combined with the oblique foliation of the quartz in the matrix, show resemblance to mylonites with an S–C fabric as suggested by Lister and Snoke (1984). However, in the studied examples of fish-shaped structures in other

minerals, the oblique foliation is in some cases destroyed by static recrystallisation (e.g. Fig. 12e), or the mylonitic foliation is not well developed. In all these cases, the fish-shape and the shape-preferred orientation are nevertheless very similar. These observations imply that this combination of shape and shape-preferred orientation of natural porphyroclasts can be developed when flow is partitioned in microshear zones.

Acknowledgements

The help of M. Müller with the microprobe analysis is greatly appreciated. H. Roig provided the sample with K-feldspar fish from the Espinhaço Belt. Rodrigo Peternel helped with the measurements of the mica fish and provided samples for Figs. 6 and 11b. We thank Neil Mancktelow, Kazuhiko Ishii and Simon Hanmer for constructive reviews. The authors acknowledge the collaborative program PROBAL (415-br-probral) with participation by DAAD from Germany and by CAPES from Brazil, for financial support. StG also thanks the German Research Foundation DFG (GRK 392/1) for financial support. RAJT acknowledges financial support from CNPq.

References

Azor, A., Ferando Simancas, J., Exposito, I., Gonzalez Lodeiro, F., Martinez Poyatos, D.J., 1997. Deformation of garnets in a low-grade shear zone. Journal of Structural Geology 19, 1137–1148.

Bell, T.H., Etheridge, M.A., 1973. Microstructure of mylonites and their descriptive terminology. Lithos 6, 337–348.

Berthé, D., Choukroune, P., Jegouzo, P., 1979. Orthogneiss, mylonite and non-coaxial deformation of granites: the example of the South Armorican shear zone. Journal of Structural Geology 1, 31–42.

Bestmann, M., 1999. Lattice diffusion creep as a possible deformation mechanism for quartz porphyroclasts within a calcite marble shear zone. Abstract Volume Deformation Mechanisms, Rheology, Microstructures, 69.

Bestmann, M., Kunze, K., Matthews, A., 2000. Evolution of a calcite marble shear complex on Thassos Island, Greece: microstructural and textural fabrics and their kinematic significance. Journal of Structural Geology 22, 1789–1807.

Den Brok, B., Kruhl, J.H., 1996. Ductility of garnet as an indicator of extremely high temperature deformation: discussion. Journal of Structural Geology 18, 1369–1373.

Echecopar, A., 1977. A plane kinematic model of progressive deformation in a polycrystalline aggregate. Tectonophysics 39, 121–139.

Eisbacher, G.H., 1970. Deformation mechanisms of mylonitic rocks and fractured granulites in Cobequid Mountains, Nova Scotia, Canada. Geological Society of America Bulletin 81, 2009–2020.

Etheridge, M.A., Hobbs, B.E., 1974. Chemical and deformation controls on recrystallisation of mica. Contributions to Mineralogy and Petrology 43, 111–124.

Ghosh, S.K., Ramberg, H., 1976. Reorientation of inclusions by combinations of pure and simple shear. Tectonophysics 34, 1–70.

Goodwin, L.B., Wenk, H.-R., 1995. Development of phyllonite from granodiorite: mechanisms of grain-size reduction in the Santa Rosa mylonite zone, California. Journal of Structural Geology 17, 689–707.

Gower, R.J.W., Simpson, C., 1992. Phase boundary mobility in naturally deformed, high-grade quartzofeldspatic rocks: evidence for diffusional creep. Journal of Structural Geology 14, 301–313.

Hanmer, S., 1990. Natural rotated inclusions in nonideal shear. Tectonophysics 176, 245–255.

Hirth, G., Teyssier, C., Dunlap, W.J., 2001. An evaluation of quartzite flow laws based on comparisons between experimentally and naturally deformed rocks. International Journal of Earth Sciences 90, 77–87.

Ishii, K., Sawaguchi, T., 2002. Lattice- and shape-preferred orientation of orthopyroxene porphyroclasts in peridotites: an application of two-dimensional numerical modelling. Journal of Structural Geology 24, 517–530.

Jeffery, G.B., 1922. The motion of ellipsoidal particles immersed in a viscous fluid. Proceedings of the Royal Society of London Series A 102, 161–179.

Ji, S., Martignole, J., 1994. Ductility of garnet as an indicator of extremely high temperature deformation. Journal of Structural Geology 16, 985–996.

Lister, G.S., Snoke, A.W., 1984. S–C mylonites. Journal of Structural Geology 6, 616–638.

Mancktelow, N.S., Arbaret, L., Pennacchioni, G., 2002. Experimental observations on the effect of interface slip on rotation and stabilisation of rigid particles in simple shear and a comparison with natural mylonites. Journal of Structural Geology 24, 567–585.

Mares, V.M., Kronenberg, A.K., 1993. Experimental deformation of muscovite. Journal of Structural Geology 15, 1061–1075.

Marques, F.G., Cobbold, P.R., 1995. Development of highly-cylindrical folds around rigid ellipsoidal inclusions in bulk simple shear regimes: natural examples and experimental modelling. Journal of Structural Geology 17, 598–602.

Marques, F.G., Coelho, S., 2001. Rotation of rigid elliptical cylinders in viscous simple shear flow: analogue experiments. Journal of Structural Geology 23, 609–617.

Masuda, T., Michibayashi, K., Ohta, H., 1995. Shape preferred orientation of rigid particles in a viscous matrix: reevaluation to determine kinematic parameters of ductile deformation. Journal of Structural Geology 17, 115–129.

Means, W.D., 1981. The concept of steady-state foliation. Tectonophysics 78, 179–199.

Niemeijer, A.R., Spiers, C.J., 2002. Compaction creep of quartz-muscovite mixtures at 500 °C: preliminary results on the influence of muscovite on pressure solution. In: De Meer, S., Drury, M.R., De Bresser, J.H.P., Pennock, G.M. (Eds.), Deformation Mechanisms, Rheology And Tectonics: Current Status and Future Perspectives. Geological Society, London, Special Publications, vol. 200, pp. 61–71.

Oliver, D.H., Goodge, J.W., 1996. Leucoxene fish as a micro-kinematic indicator. Journal of Structural Geology 18, 1493–1497.

Paciullo, F.V.P., Ribeiro, A., Andreis, R.R., 1993. Reconstrução de uma bacia fragmentada: o caso do Ciclo Deposicional Andrelândia. Simpósio do Cráton do São Francisco, 2, Salvador, pp. 224–226.

Passchier, C.W., 1985. Water-deficient mylonite zones—an example from the Pyrenees. Lithos 18, 115–127.

Passchier, C.W., 1987. Stable positions of rigid objects in non-coaxial flow—a study in vorticity analysis. Journal of Structural Geology 9, 679–690.

Passchier, C.W., 1994. Mixing in flow perturbations: a model for development of mantled porphyroclasts in mylonites. Journal of Structural Geology 16, 733–736.

Passchier, C.W., Simpson, C., 1986. Porphyroclast systems as kinematic indicators. Journal of Structural Geology 8, 831–843.

Passchier, C.W., Trouw, R.A.J., 1996. Microtectonics. Springer Verlag, Berlin. 289 pp.

Passchier, C.W., ten Brink, C.E., Bons, P.D., Sokoutis, D., 1993. Delta-objects as a gauge for stress sensitivity of strain rate in mylonites. Earth and Planetary Science Letters 120, 239–245.

Pennacchioni, G., Di Toro, G., Mancktelow, N.S., 2001. Strain-insensitive preferred orientation of porphyroblasts in Mont Mary mylonites. Journal of Structural Geology 23, 1281–1298.

Ribeiro, A., Trouw, R.A.J., Andreis, R.R., Paciullo, F.V.P., Valença, J.G., 1995. Evolução das bacias Proterozóicas e o termo-tectonismo Brasiliano na margem sul do Cráton do São Francisco. Revista Brasileira de Geociências 25, 235–248.

Simpson, C., Schmid, S.M., 1983. An evaluation of criteria to deduce the sense of movement in sheared rocks. Geological Society of America Bulletin 94, 1281–1288.

Simpson, C., Wintch, R.P., 1989. Evidence for deformation-induced K-feldspar replacement by myrmekite. Journal of Metamorphic Geology 7, 261–275.

ten Grotenhuis, S.M., Passchier, C.W., Bons, P.D., 2002. The influence of strain localisation on the rotational behaviour of rigid objects in experimental shear zones. Journal of Structural Geology 24, 485–499.

Trouw, R.A.J., Ribeiro, A., Paciullo, F.V., 1983. Geologia estrutural dos grupos São João del Rei, Carrancas e Andrelândia, Sul de Minas Gerais. Anais da Academia Brasileira de Ciências 55, 71–85.

Trouw, R.A.J., Heilbron, M., Ribeiro, A., Paciullo, F.V.P., Valeriano, C.M., Almeida, J.C.H., Tupinambá, M., Andreis, R.R., 2000. The central segment of the Ribeira Belt. In: Cordani, U.G., Milani, E.J., Thomaz Filho, A., Campos, D.A. (Eds.), Tectonic Evolution of South America. 31st International Geological Congress, Rio de Janeiro, Brazil, pp. 287–311.

Tullis, J., Yund, R.A., 1991. Diffusion creep in feldspar aggregates: experimental evidence. Journal of Structural Geology 13, 987–1000.

Vernon, R.H., 1986. Evaluation of the "quartz eye" hypothesis. Economic Geology 81, 1520–1527.

Wenk, H.-R., Pannetier, J., 1990. Texture development in deformed granodiorites from the Santa Rosa mylonite zone, southern California. Journal of Structural Geology 12, 177–184.

Williams, M.L., Burr, J.L., 1994. Preservation and evolution of quartz phenocrystsin deformed rhyolites from the Proterozoic of southwestern North America. Journal of Structural Geology 16, 203–221.